



All-optical switching in a medium of a four-level vee-cascade atomic medium

Khoa Dinh Xuan¹ · Ai Nguyen Van¹ · Dong Hoang Minh² · Doai Le Van¹ · Bang Nguyen Huy¹ 

Received: 14 February 2019 / Accepted: 20 December 2021

© The Author(s), under exclusive licence to Springer Science+Business Media, LLC, part of Springer Nature 2022

Abstract

We proposed a model for all-optical switching in a medium consisting of four-level vee-cascade atomic systems excited by coupling, probe, and signal fields. It is shown that, by changing the intensity or the frequency of the signal field, the medium can be actively switched between either electromagnetically induced transparency or electromagnetically induced absorption, which has behavior of all-optical switching. As a result, a *cw* probe field is switched into square pulses by modulating the intensity or the frequency of the signal light. Furthermore, width of the square probe pulses can be controlled by tuning the switching period of the signal field. Such a tuneable all-optical switching is useful for finding related applications in optic communications and optical storage devices.

Keywords Optical bistability · Optical switches · Coherent optical communications

1 Introduction

All-optical switch is an important component in high-speed optical communication networks and quantum computing (Ishikawa 2008). Over the last few decades, all-optical switching based on optical bistability in two-level atomic systems was studied. However, applications of the two-level atomic system is limited due to strong resonant absorption and only one optical field is employed for both applying and switching, thus lack of control for switching intensity thresholds. The advent of EIT (Imamoğlu and Harris 1989; Boller et al. 1991; Fleischhauer et al. 2005; Doai et al. 2014; Khoa et al. 2016, 2017a) has created transparent media whose optical properties can be controlled by the external fields. Due to very steep dispersion in transparent spectral region, therefore light pulses can propagate with very small group velocities (Hau et al. 1999; Anh et al. 2018a, 2018b), the medium can achieve giant Kerr nonlinearities (Wang et al. 2001; Khoa et al. 2014; Hamedi et al. 2016; Doai et al. 2019), and optical soliton is also easily achieved with low intensity (Huang et al. 2006; Si et al. 2010; Chen et al. 2014; Khoa et al. 2017b; Dong et al. 2018).

✉ Bang Nguyen Huy
bangnh@vinhuni.edu.vn

¹ Vinh University, 182 Le Duan Street, Vinh, Vietnam

² Ho Chi Minh City University of Food Industry, Ho Chi Minh City, Vietnam

In recent years, optical switching at low-light intensities based on the quantum interferences has attracted extensively attentions because of its interesting applications, such as high responsibly speed and low switching power compared with electro-optical switching and the switching of silicon waveguides or fiber-based systems. Several approaches for optical switching in EIT media were proposed theoretically and demonstrated experimentally in three-level atomic systems of Λ (Λ), vee (V) and ladder (Ξ) configurations, such as all-optical switching based on optical bistability (Wang et al. 2002; Jafarzadeh 2017) and all-optical switching in pulse mode (Schmidt and Ram 2000; Fountoulakis et al. 2010; Dong et al. 2019; Dong and Bang 2019).

In addition to the three-level systems, EIT has also been implemented in four-level atomic systems including N-type ($\Lambda + V$) (Islam et al. 2017), inverted Y-type ($\Lambda + \Xi$) (Joshi and Xiao 2003, 2004, 2005), tripod-type ($\Lambda + \Lambda$) (Yang et al. 2009) and $V + \Xi$ -type (Bharti and Natarajan 2015) configurations. The advantage of four-level atomic systems is that it can be generated double-EIT windows and can be switched between EIT and EIA by signal field or external magnetic field. This provides a new way to control the light propagation between fast and slow modes (Asadpour 2017; Bharti and Natarajan 2017), switch between optical bistability and optical multistability (Asadpour and Soleimani 2016a, b), and create optical switches. For example, Li et al. (2010) studied the dynamics of pulse propagation and magneto-optic dual switching in a four-level inverted-Y atomic medium via switching on and off an external magnetic field, Qi et al. (2013) presented the propagation dynamics of weak twin laser pulses and a dual-optical switching scheme in four-level semiconductor quantum dots of diamond configuration via adjusting the intensities of the control fields and the relative phase of the fields, Antón et al. (2006) showed the optical bistable response and all-optical switching in a four-level tripod-type atomic system can be obtained by changing the intensity of one of the control fields, and Sheng et al. (2011) experimentally demonstrated that an all-optical switching can be achieved by simply choosing different probe frequencies in an N-type atom-cavity system.

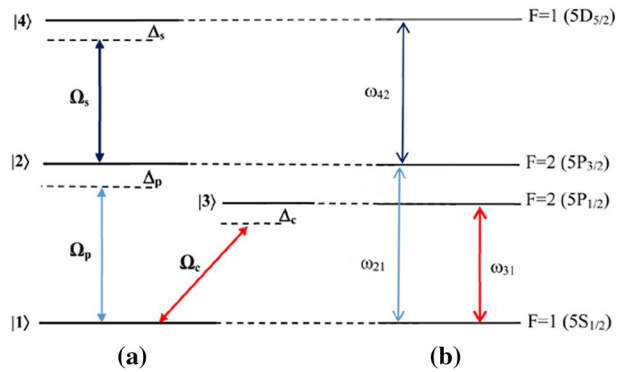
Although all-optical switching in pulse mode have been studied for several four-level configurations but there still lacks study for the four-level $V + \Xi$ system. As suggested by Bharti et al. (2015), the four-level $V + \Xi$ configuration could be actively switched between EIT and EIA modes. From the physics point of view, the medium of such behaviour is favourable to generate all-optical switching.

In this work we propose to use a four-level $V + \Xi$ scheme for all-optical switching in pulse mode by numerically solving Maxwell-Bloch equations on a space–time grid. The switching of the probe laser according to the frequency and intensity of the signal laser has been considered. The advantage of this model is that we can easily switch between EIT and EIA by adjusting the frequency or intensity of the signal laser so that it is easy to create optical switching for a weak probe pulse. More, this excitation scheme can be used to excite Rydberg states having long life-time (few ms) in which light pulse can be manipulated and slowed down to few mm/s (Bharti and Natarajan 2017).

2 Theoretical model

We consider an atomic medium consists of four-level vee-cascade excitation scheme having a ground state $|1\rangle$ and three excited states $|2\rangle$, $|3\rangle$ and $|4\rangle$, as shown in Fig. 1a. An optical probe field with frequency ω_p and Rabi frequency Ω_p drives the transition $|1\rangle \leftrightarrow |2\rangle$, while the transition $|1\rangle \leftrightarrow |3\rangle$ and $|2\rangle \leftrightarrow |4\rangle$ are excited by coupling (frequency ω_c) and signal (frequency

Fig. 1 a The four-level atomic vee-cascade scheme and **b** Relevant energy level diagram of ^{87}Rb atom



ω_s) optical fields with Rabi frequency Ω_c and Ω_s , respectively. The decay rates from the states $|2\rangle$ and $|3\rangle$ to the ground state $|1\rangle$, and from the excited state $|4\rangle$ to the state $|2\rangle$ denoted by γ_{21} , γ_{31} and γ_{42} , respectively.

Using the rotating-wave and the electric dipole approximations, the total Hamiltonian of the system in the interaction picture can be written as (in units \hbar).

$$H = \begin{bmatrix} 0 & -\Omega_p^* & -\Omega_c^* & 0 \\ -\Omega_p & \Delta_p & 0 & -\Omega_s^* \\ -\Omega_c & 0 & \Delta_c & 0 \\ 0 & -\Omega_s & 0 & \Delta_p + \Delta_s \end{bmatrix}, \tag{1}$$

where $\Delta_p = \omega_{21} - \omega_p$, $\Delta_c = \omega_{31} - \omega_c$, and $\Delta_s = \omega_{42} - \omega_s$ are frequency detunings of the probe, coupling, and signal fields, respectively. The dynamical evolution of the system can be described by the Liouville equation:

$$\frac{\partial \rho}{\partial t} = -i[H, \rho] + \Lambda \rho, \tag{2}$$

where $\Lambda \rho$ represents the decaying processes. For the four-level vee-cascade system, the density matrix equations in Eq. (2) are decomposed as:

$$\frac{\partial \rho_{11}}{\partial t} = \gamma_{21} \rho_{22} + \gamma_{31} \rho_{33} + i\Omega_p^* \rho_{21} - i\Omega_p \rho_{12} + i\Omega_c^* \rho_{31} - i\Omega_c \rho_{13}, \tag{3a}$$

$$\frac{\partial \rho_{22}}{\partial t} = -\gamma_{21} \rho_{22} + \gamma_{42} \rho_{44} - i\Omega_p^* \rho_{21} + i\Omega_p \rho_{12} + i\Omega_s^* \rho_{42} - i\Omega_s \rho_{24}, \tag{3b}$$

$$\frac{\partial \rho_{33}}{\partial t} = -\gamma_{31} \rho_{33} - i\Omega_c^* \rho_{31} + i\Omega_c \rho_{13}, \tag{3c}$$

$$\frac{\partial \rho_{44}}{\partial t} = -\gamma_{42} \rho_{44} - i\Omega_s^* \rho_{42} + i\Omega_s \rho_{24}, \tag{3d}$$

$$\frac{\partial \rho_{21}}{\partial t} = -\left(i\Delta_p + \frac{\gamma_{21}}{2}\right)\rho_{21} + i\Omega_p(\rho_{11} - \rho_{22}) - i\Omega_c\rho_{23} + i\Omega_s^*\rho_{41}, \quad (3e)$$

$$\frac{\partial \rho_{31}}{\partial t} = -\left(i\Delta_c + \frac{\gamma_{31}}{2}\right)\rho_{31} + i\Omega_c(\rho_{11} - \rho_{33}) - i\Omega_p\rho_{32}, \quad (3f)$$

$$\frac{\partial \rho_{41}}{\partial t} = -\left(i(\Delta_p + \Delta_s) + \frac{\gamma_{42}}{2}\right)\rho_{41} - i\Omega_p\rho_{42} - i\Omega_c\rho_{43} + i\Omega_s\rho_{21}, \quad (3g)$$

$$\frac{\partial \rho_{32}}{\partial t} = -\left(i(\Delta_c - \Delta_p) + \frac{\gamma_{21} + \gamma_{31}}{2}\right)\rho_{32} - i\Omega_p^*\rho_{31} + i\Omega_c\rho_{12} - i\Omega_s\rho_{34}, \quad (3h)$$

$$\frac{\partial \rho_{42}}{\partial t} = -\left(i\Delta_s + \frac{\gamma_{21} + \gamma_{42}}{2}\right)\rho_{42} - i\Omega_p^*\rho_{41} + i\Omega_s(\rho_{22} - \rho_{44}), \quad (3i)$$

$$\frac{\partial \rho_{43}}{\partial t} = -\left(i(\Delta_p + \Delta_s - \Delta_c) + \frac{\gamma_{31} + \gamma_{42}}{2}\right)\rho_{43} + i\Omega_c^*\rho_{41} + i\Omega_s\rho_{23}. \quad (3j)$$

where the matrix elements obey conjugated and normalized conditions, namely $\rho_{ij} = \rho_{ij}^*$ ($i \neq j$), and $\rho_{11} + \rho_{22} + \rho_{33} + \rho_{44} = 1$, respectively.

3 Results and discussions

In order to illustrate the model of all-optical switching, we apply to cold ^{87}Rb atomic medium in where the states $|1\rangle, |2\rangle, |3\rangle$ and $|4\rangle$ correspond to the levels $|5S_{1/2}, F=|1\rangle, |5P_{3/2}, F'=|2\rangle, |5P_{1/2}, F'=|2\rangle, |5D_{5/2}, F''=|1\rangle$ as depicted in Fig. 1b. The atom and laser parameters given by Steck (2021): $\gamma_{21} = 6.1$ MHz, $\gamma_{31} = 5.9$ MHz, $\gamma_{42} = 0.68$ MHz, $\lambda_p = 780$ nm, $\lambda_c = 795$ nm, and $\lambda_s = 776$ nm.

3.1 Switching between EIT and EIA

First of all, we consider the influence of the switching signal field on the absorption and dispersion properties of medium for the probe field in the presence of coupling field at the steady regime. The linear susceptibility χ of the atomic medium for the probe light field relates to the matrix element ρ_{21} determined by Doai et al. (2014):

$$\chi = 2 \frac{Nd_{21}}{\epsilon_0 E_p} \rho_{21}. \quad (4)$$

where the matrix element ρ_{21} is solved numerically from set of Eqs. (3a–3j). The imaginary χ'' and real χ' parts of the linear susceptibility represent the absorption and dispersion, respectively. In Fig. 2, we plotted the absorption $\text{Im}(\rho_{21})$ and dispersion $\text{Re}(\rho_{21})$ versus the frequency detuning Δ_p for the cases of absence ($\Omega_s = 0$) and presence ($\Omega_s = 9\gamma_{21}$) signal field. Here we used resonant conditions $\Delta_c = \Delta_s = 0$ and $\Omega_p = 0.01\gamma_{21}$, $\Omega_c = 9\gamma_{21}$.

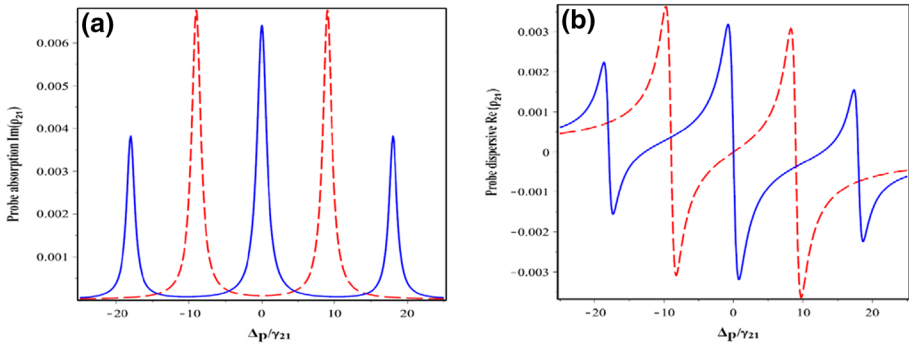


Fig. 2 Variations of probe absorption **(a)** and dispersion **(b)** versus the probe detuning Δ_p for the given values of $\Omega_p = 0.01\gamma_{21}$, $\Omega_c = 9\gamma_{21}$, $\Delta_c = 0$, $\Delta_s = 0$, $\Omega_s = 9\gamma_{21}$ when the switching field off (dashed) or on (solid) at Rabi frequency

As shown in Fig. 2, the absorption and dispersion spectra of the probe field depend sensitively on the ON or OFF mode of the signal field. Indeed, when switching field OFF, $\Omega_s = 0$ (dashed lines), the absorption of the probe field can be suppressed thus the medium becomes completely transparent to the probe field at line center, which the corresponding dispersion profile has a positive slope near zero detuning (dashed line Fig. 2b) hence the probe light is slowed down. However, when the signal field is turns on, $\Omega_s = \Omega_c = 9\gamma_{21}$, the medium is switched from transparent to a complete absorbing mode (EIA) at the line center. Furthermore, the absorption profile for the probe field is switched from single transparency window centered at $\Delta_p = 0$ to a double-transparency window located at $\Delta_p = \pm \Omega_c$. The corresponding dispersion profile has a negative slope near zero detuning (solid line Fig. 2b), thus the medium speeds up group velocity of the probe light.

3.2 All-optical switching

Now we extend our consideration from the steady to a dynamical regime. Under the slowly-varying envelope and rotating-wave approximations, evolution of the probe field is represented by the following wave equation (Khoa et al. 2017b):

$$\frac{\partial \Omega_p(z, t)}{\partial z} + \frac{1}{c} \frac{\partial \Omega_p(z, t)}{\partial t} = i\alpha \gamma_{21} \rho_{21}(z, t), \tag{5}$$

here $\alpha = \frac{\omega_p N |d_{21}|^2}{4\epsilon_0 c \hbar \gamma_{21}}$ is the propagation constant. For a convenience, we represent Rabi frequency of the probe field by $\Omega_p(z, t) = \Omega_{p0} f(z, t)$, where Ω_{p0} is a real constant indicating the maximal value of the Rabi frequency at the entrance (*i.e.*, at $z=0$), and $f(z, t)$ is a dimensionless spatiotemporal pulse-shaped function. In a moving frame with $\xi = z$ and $\tau = t - z/c$, the optical Bloch matrix Eqs. (3a–3j) for the density matrix elements $\rho_{ij}(\xi, \tau)$ and Maxwell’s wave Eq. (5) for the probe field $f(\xi, \tau)$ can be rewritten by:

$$\frac{\partial \rho_{11}}{\partial \tau} = \gamma_{21} \rho_{22} + \gamma_{31} \rho_{33} + i\Omega_{p0} f^*(\xi, \tau) \rho_{21} - i\Omega_{p0} f(\xi, \tau) \rho_{12} + i\Omega_c^* \rho_{31} - i\Omega_c \rho_{13}, \tag{6a}$$

$$\frac{\partial \rho_{22}}{\partial \tau} = -\gamma_{21}\rho_{22} + \gamma_{42}\rho_{44} - i\Omega_{p0}f^*(\xi, \tau)\rho_{21} + i\Omega_{p0}f(\xi, \tau)\rho_{12} + i\Omega_s^*\rho_{42} - i\Omega_s\rho_{24}, \quad (6b)$$

$$\frac{\partial \rho_{33}}{\partial \tau} = -\gamma_{31}\rho_{33} - i\Omega_c^*\rho_{31} + i\Omega_c\rho_{13}, \quad (6c)$$

$$\frac{\partial \rho_{44}}{\partial \tau} = -\gamma_{42}\rho_{44} - i\Omega_s^*\rho_{42} + i\Omega_s\rho_{24}, \quad (6d)$$

$$\frac{\partial \rho_{21}}{\partial \tau} = -\left(i\Delta_p + \frac{\gamma_{21}}{2}\right)\rho_{21} + i\Omega_{p0}f(\xi, \tau)(\rho_{11} - \rho_{22}) - i\Omega_c\rho_{23} + i\Omega_s^*\rho_{41}, \quad (6e)$$

$$\frac{\partial \rho_{31}}{\partial \tau} = -\left(i\Delta_c + \frac{\gamma_{31}}{2}\right)\rho_{31} + i\Omega_c(\rho_{11} - \rho_{33}) - i\Omega_{p0}f(\xi, \tau)\rho_{32}, \quad (6f)$$

$$\frac{\partial \rho_{41}}{\partial \tau} = -\left(i(\Delta_p + \Delta_s) + \frac{\gamma_{42}}{2}\right)\rho_{41} - i\Omega_{p0}f(\xi, \tau)\rho_{42} - i\Omega_c\rho_{43} + i\Omega_s\rho_{21}, \quad (6g)$$

$$\frac{\partial \rho_{32}}{\partial \tau} = -\left(i(\Delta_c - \Delta_p) + \frac{\gamma_{21} + \gamma_{31}}{2}\right)\rho_{32} - i\Omega_{p0}f^*(\xi, \tau)\rho_{31} + i\Omega_c\rho_{12} - i\Omega_s\rho_{34}, \quad (6h)$$

$$\frac{\partial \rho_{42}}{\partial \tau} = -\left(i\Delta_s + \frac{\gamma_{21} + \gamma_{42}}{2}\right)\rho_{42} - i\Omega_{p0}f^*(\xi, \tau)\rho_{41} + i\Omega_s(\rho_{22} - \rho_{44}), \quad (6i)$$

$$\frac{\partial \rho_{43}}{\partial \tau} = -\left(i(\Delta_p + \Delta_s - \Delta_c) + \frac{\gamma_{31} + \gamma_{42}}{2}\right)\rho_{43} + i\Omega_c^*\rho_{41} + i\Omega_s\rho_{23}, \quad (6j)$$

$$\frac{\partial f(\xi, \tau)}{\partial(\alpha\xi)} = i\frac{\gamma_{21}}{\Omega_{p0}}\rho_{21}(\xi, \tau). \quad (6k)$$

In the following, we solve numerically the set of Eqs. (6a–k) on a space–time grid by using a combination of the four-order Runge–Kutta and finite difference methods which were developed from our previous work (Khoa et al. 2017b). We assumed the initial condition is all atoms in the ground state $|1\rangle$ whereas the boundary condition is the probe pulse having a Gaussian-type shape $f(\xi = 0, \tau) = \exp[-(\ln 2)(\tau - 30)^2/\tau_0^2]$, with $\tau_0 = 6/\gamma_{21}$ is the temporal width of the pulse at the entrance of the medium.

In Fig. 3 we plotted spatiotemporal evolution of intensity (square of magnitude) of the probe field at different intensities of the signal field when $\Omega_c = 9\gamma_{21}$, $\Delta_c = \Delta_s = \Delta_p = 0$. It is shown that the OFF or ON mode of the signal field affects sensitively on the probe pulse absorption. When the signal field OFF (i.e., $\Omega_s = 0$), the atomic medium is transparent to the probe pulse, namely, the probe pulse remains unchanged over a long traveling distance (Fig. 3a). As the signal field ON at $\Omega_s = \Omega_c = 9\gamma_{21}$, the probe pulse can be absorbed completely, even in a noticeably short propagation distance (see Fig. 3b). This strong absorption associates with EIA phenomenon, as indicated in Fig. 2a.

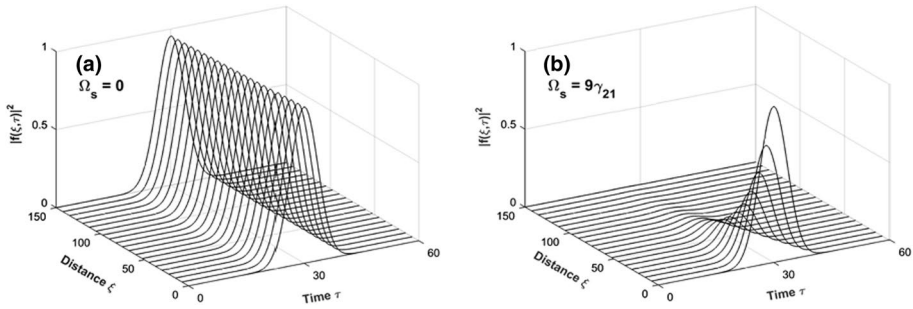


Fig. 3 Space–time evolution of the normalized probe intensity at $\Omega_s=0$ (a) and $\Omega_s=9\gamma_{21}$ (b). Other used parameters are $\Omega_{0p}=0.01\gamma_{21}$, $\Omega_c=9\gamma_{21}$, $\Delta_p=\Delta_c=\Delta_s=0$; time τ and propagation distance ξ are calculated in units of γ_{21}^{-1} and α^{-1} , respectively

Consequently, by switching intensity of the signal field the medium can be switched to either EIT or EIA for the probe pulse.

In Fig. 4, we plotted the normalized probe field intensity for different values of the signal detuning Δ_s while keeping other parameters at $\Delta_p=0$, $\Delta_c=9\gamma_{21}$, $\Omega_{0p}=0.01\gamma_{21}$, $\Omega_c=8\gamma_{21}$, and $\Omega_s=9\gamma_{21}$. When $\Delta_s=0$, the medium is almost transparent for probe pulse (Fig. 4a) whereas it absorbs completely probe pulses as Δ_s increasing to a value $\Delta_s=10\gamma_{21}$ (see Fig. 4b). From this feature one can conclude that the medium can be switched from EIT to EIA by tuning frequency of the signal field.

Next, we consider a possible way to realize all-optical switching for the probe field by tuning parameters of the signal field, as shown in Fig. 5. Here, the probe field (*solid lines*) is assumed to be a continuous wave (*cw*) whereas the switching signal field (*dashed lines*) to be nearly-square pulses with smooth rising and falling edges. The signal field is switched by the following rules:

$$\Omega_s(\tau) = \Omega_{s0} \{1 - 0.5[\tanh 0.4(\tau - 20) + \tanh 0.4(\tau - 45) - \tanh 0.4(\tau - 70) + \tanh 0.4(\tau - 95)]\}, \tag{7}$$

$$\Omega_s(\tau) = \Omega_{s0} \{1 - 0.5[\tanh 0.2(\tau - 40) + \tanh 0.2(\tau - 90) - \tanh 0.2(\tau - 140) + \tanh 0.2(\tau - 190)]\}. \tag{8}$$

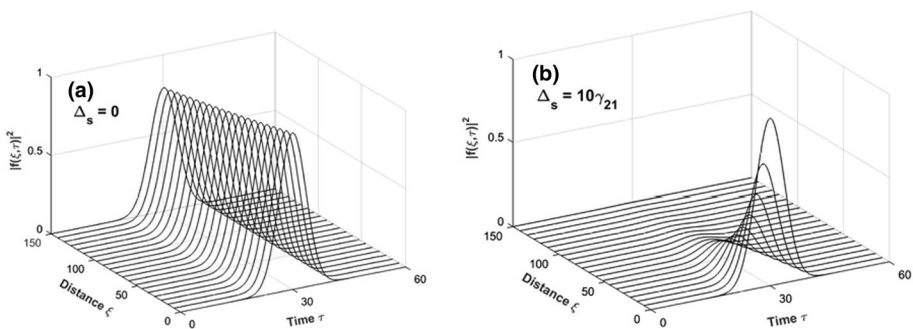


Fig. 4 The space–time evolution of normalized probe field intensity at $\Delta_s=0$ (a) and $\Delta_s=10\gamma_{21}$ (b). Other parameters are $\Omega_{0p}=0.01\gamma_{21}$, $\Omega_c=8\gamma_{21}$, $\Omega_s=9\gamma_{21}$, $\Delta_p=0$, $\Delta_c=9\gamma_{21}$; time τ and propagation distance ξ are calculated in units of γ_{21}^{-1} and α^{-1} , respectively

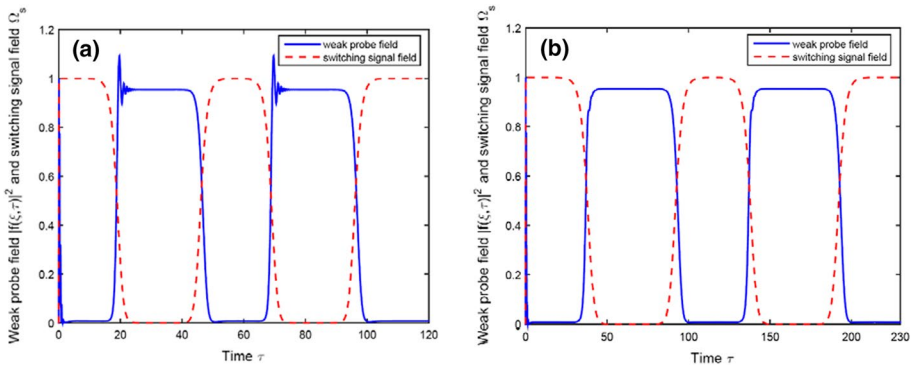


Fig. 5 Time evolution of a *cw* probe field (solid line) at $\xi=150/\alpha$ when the signal field (dashed lines) switched at approximate period $50/\gamma_{21}$ (a) and $100/\gamma_{21}$ (b). Other parameters are $f(\xi=0, \tau)=1, \Omega_{p0}=0.01\gamma_{21}, \Omega_{s0}=\Omega_c=9\gamma_{21}, \Delta_p=0, \Delta_c=0, \Delta_s=0$; time τ is calculated in units of γ_{21}^{-1}

here the intensity of the signal field in Eqs. (7) or (8) is switched with approximate period $50/\gamma_{21}$ and $100/\gamma_{21}$, respectively. In Fig. 5 we plotted the switching field when the amplitude of the signal field is normalized by its peak value $\Omega_{s0}=9\gamma_{21}$. Figure 5 shows that the switching periods of both probe and signal fields are the same. Furthermore, the probe transmission is switched to the ON or OFF mode when the intensity of the signal field is OFF or ON, respectively. On the other hand, oscillations at the front edge of the probe pulse can be extinguished when increasing width of the signal pulse (Fig. 5b).

In Fig. 6, we consider the dynamics of the *cw* probe field (solid lines) under modulating frequency of the signal field (dashed lines). Here, frequency detuning of the probe field is chosen as a nearly-square pulse with smooth rising and falling edges as follows:

$$D_s(\tau) = -D_{s0} \{1 - 0.5[\tanh 0.4(\tau - 20) + \tanh 0.4(\tau - 45) - \tanh 0.4(\tau - 70) + \tanh 0.4(\tau - 95)]\}, \tag{9}$$

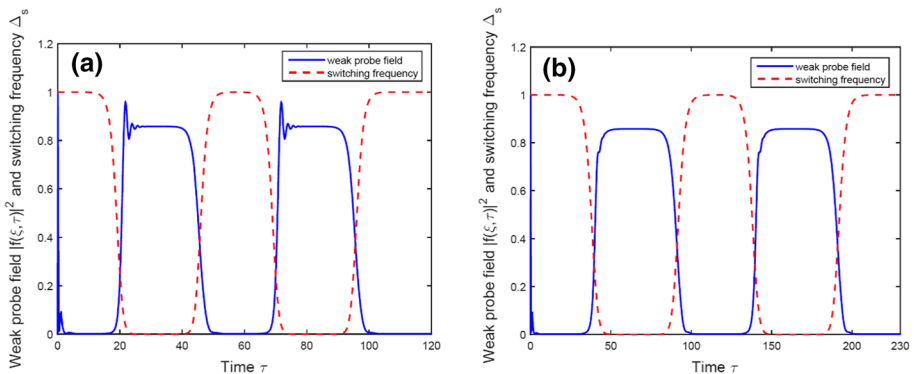


Fig. 6 Time evolution of a *cw* probe field (solid line) at $\xi=150/\alpha$ when the signal field (dashed lines) switched at approximate period $50/\gamma_{21}$ (a) and $100/\gamma_{21}$ (b). Other parameters are $f(\xi=0, \tau)=1, \Omega_{p0}=0.01\gamma_{21}, \Omega_c=8\gamma_{21}, \Omega_s=9\gamma_{21}, \Delta_p=0, \Delta_c=9\gamma_{21}, \Delta_{s0}=10\gamma_{21}$; time τ is calculated in units of γ_{21}^{-1}

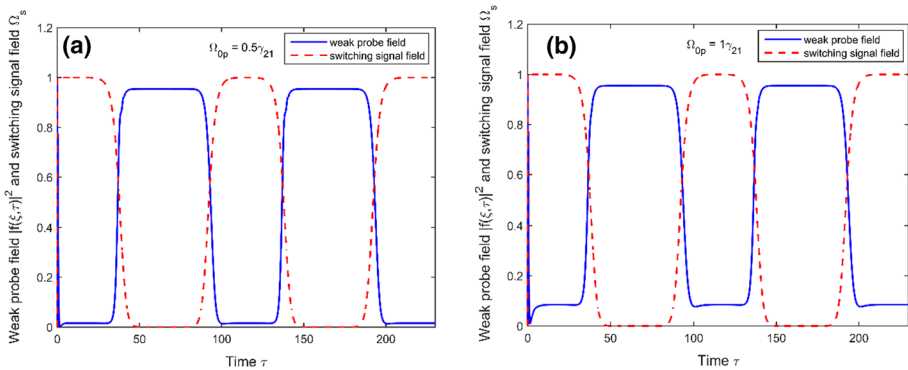


Fig. 7 Time evolution of a cw probe field (solid line) at $\xi = 150/\alpha$ when the signal field (dashed lines) switched at approximate period $100/\gamma_{21}$, and the probe field intensity $\Omega_{p0} = 0.5\gamma_{21}$ (a) and $\Omega_{p0} = 1\gamma_{21}$ (b). Other parameters given as same as those in Fig. 5

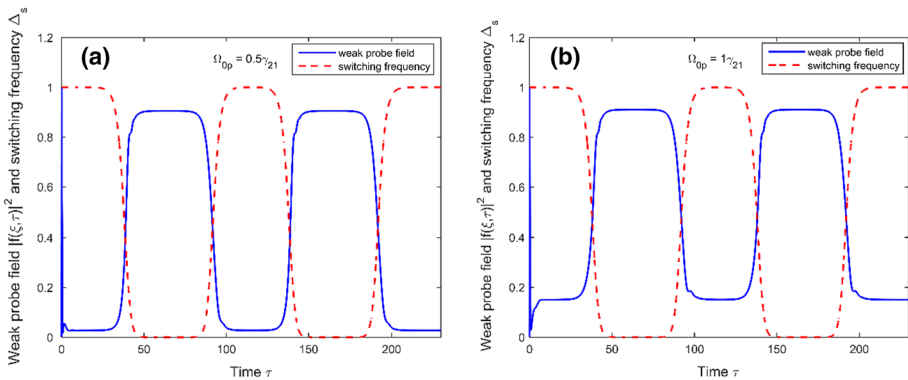


Fig. 8 Time evolution of a cw probe field (solid line) at $\xi = 150/\alpha$ when the signal field (dashed lines) switched at approximate period $100/\gamma_{21}$, and the probe field intensity $\Omega_{p0} = 0.5\gamma_{21}$ (a) and $\Omega_{p0} = 1\gamma_{21}$ (b). Other parameters given as same as those in Fig. 6

$$D_s(\tau) = D_{s0} \{1 - 0.5[\tanh 0.2(\tau - 40) + \tanh 0.2(\tau - 90) - \tanh 0.2(\tau - 140) + \tanh 0.2(\tau - 190)]\}. \tag{10}$$

here the frequency detuning of the signal field in Eqs. (9) or (10) is switched with approximate period $50/\gamma_{21}$ and $100/\gamma_{21}$, respectively. In both cases, the frequency detuning is normalized by its peak value as $\Delta_{s0} = 10\gamma_{21}$. We can see that the probe transmission is switched to either ON or OFF when the frequency detuning of the signal field is switched OFF or ON, respectively. As indicated in the Sect. 3.1, the ON or OFF mode for probe field can be attributed from EIT or EIA mode of the medium, respectively.

Finally, we consider the behavior of optical switching according as intensity (Fig. 7) and the frequency (Fig. 8) of the signal field in strong probe regime. Figures 7 and 8 show the cases of Figs. 5b and 6b, respectively, while the probe intensity is increased to $\Omega_{p0} = 0.5\gamma_{21}$ (a) and $\Omega_{p0} = 1\gamma_{21}$ (b). From these figures we can see that when intensity of the probe field is of the same order with the coupling field, the switching efficiency decreases. To explain

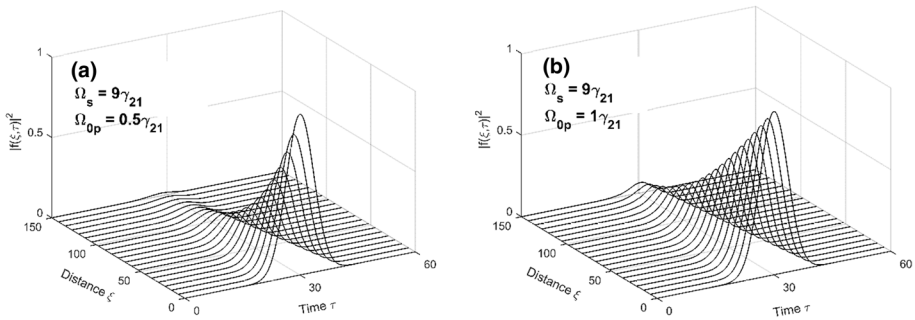


Fig. 9 Space–time evolution of the normalized probe intensity at $\Omega_s = \Omega_c = 9\gamma_{21}$, and $\Omega_{op} = 0.5\gamma_{21}$ (a) and $\Omega_{op} = 1\gamma_{21}$ (b). Other parameters given as same as those in Fig. 3

the phenomenon, we plot spatiotemporal evolution of intensity of the probe pulse at $\Omega_s = \Omega_c = 9\gamma_{21}$, $\Delta_c = \Delta_s = \Delta_p = 0$ and $\Omega_{p0} = 0.5\gamma_{21}$ (a) and $\Omega_{p0} = 1\gamma_{21}$ (b) as shown in Fig. 9. Due to strong intensity of the probe field, its intensity will not be absorbed completely, then it may transfer to the next period, which results higher background (Figs. 7b and 8b), namely lower switching efficiency. Moreover, the strong probe pulse corresponding to self-phase modulation is formed and the switching process can be broken down gradually (Rajitha et al. 2015).

4 Conclusion

We have proposed a model of four-level vee-cascade atomic medium to realize all-optical switching for a probe light in weak and strong probe regimes. Due to quantum interferences among atomic transition paths induced by coupling, probe and signal optical fields, the medium can be switched to either EIT or EIA regime by switching the signal field to OFF or ON, respectively. As a result, an all-optical switching can be generated in which the cw probe field is switched into pulses by modulating intensity or frequency of the signal light. Furthermore, width of the probe pulses can be controlled by tuning switching period of the signal field. Such a tuneable all-optical switching is useful for finding related applications in optics communications and optical storage devices.

Funding The financial support from Vietnamese National Foundation of Science and Technology Development (NAFOSTED) under Grant No. 103.03-2017.332 and Vietnamese Ministry of Education and Training under Grant No. B2018-TDV-01SP is acknowledged.

Declarations

Conflict of interest The authors have not disclosed any competing interests.

References

Anh, N.T., Doai, L.V., Son, D.H., Bang, N.H.: Manipulating multi-frequency light in a five-level cascade EIT medium under Doppler broadening. *Optik* **171**, 721–727 (2018a)

- Anh, N.T., Doai, L.V., Bang, N.H.: Manipulating multi-frequency light in a five-level cascade-type atomic medium associated with giant self-Kerr nonlinearity. *J. Opt. Soc. Am. B* **35**, 1233–1239 (2018b)
- Antón, M.A., Calderón, O.G., Melle, S., Gonzalo, I., Carreño, F.: All-optical switching and storage in a four-level tripod-type atomic system. *Opt. Commun.* **268**, 146–154 (2006)
- Asadpour, S.H.: Goos-Hänchen shifts due to spin-orbit coupling in the carbon nanotube quantum dot nanostructures. *Appl. Opt.* **56**, 2201–2208 (2017)
- Asadpour, S.H., Soleimani, H.R.: Phase dependence of optical bistability and multistability in a four-level quantum system near a plasmonic nanostructure. *J. App. Phys.* **119**, 023102 (2016)
- Asadpour, S.H., Soleimani, H.R.: Phase dependence of optical bistability and multistability in graphene nanostructure under external magnetic field. *Las. Phys. Lett.* **13**, 015204 (2016)
- Bharti, V., Natarajan, V.: Study of a four-level system in vee + ladder configuration. *Opt. Commun.* **356**, 510–514 (2015)
- Bharti, V., Natarajan, V.: Sub- and super-luminal light propagation using a Rydberg state. *Opt. Comm.* **392**, 180–184 (2017)
- Boller, K.J., Imamoglu, A., Harris, S.E.: Observation of electromagnetically induced transparency. *Phys. Rev. Lett.* **66**, 2593 (1991)
- Chen, Y., Bai, Z., Huang, G.: Ultraslow optical solitons and their storage and retrieval in an ultracold ladder-type atomic system. *Phys. Rev. A* **89**, 023835 (2014)
- Doai, L.V., Trong, P.V., Khoa, D.X., Bang, N.H.: Electromagnetically induced transparency in five-level cascade scheme of ^{85}Rb atoms: an analytical approach. *Optik* **125**, 3666–3669 (2014)
- Doai, L.V., An, N.L.T., Khoa, D.X., Sau, V.N., Bang, N.H.: Manipulating giant cross-Kerr nonlinearity at multiple frequencies in an atomic gaseous medium. *J. Opt. Soc. Am. B* **36**, 2856–2862 (2019)
- Dong, H.M., Bang, N.H.: Controllable optical switching in a closed-loop three-level lambda system. *Phy. Scr.* **94**, 115510 (2019)
- Dong, H.M., Doai, L.V., Khoa, D.X., Bang, N.H.: Pulse propagation in an atomic medium under spontaneously generated coherence, incoherent pumping, and relative laser phase. *Opt. Commun.* **426**, 553–557 (2018)
- Dong, H.M., Nga, L.T.Y., Bang, N.H.: Optical switching and bistability in a degenerated two-level atomic medium under an external magnetic field. *Appl. Opt.* **58**, 4192–4199 (2019)
- Fleischhauer, M., Imamoglu, A., Marangos, J.P.: Electromagnetically induced transparency: optics in coherent media. *Rev. Mod. Phys.* **77**, 633 (2005)
- Fountoulakis, A., Terzis, A.F., Paspalakis, E.: All-optical modulation based on electromagnetically induced transparency. *Phys. Lett. A* **374**, 3354–3364 (2010)
- Hamed, H.R., Gharamaleki, A.H., Sahrai, M.: Colossal Kerr nonlinearity based on electromagnetically induced transparency in a five-level double-ladder atomic system. *Appl. Opt.* **22**, 5892–5899 (2016)
- Hau, L.V., Harris, S.E., Dutton, Z., Bejroozi, C.H.: Light speed reduction to 17 metres per second in an ultracold atomic gas. *Nature* **397**, 594–598 (1999)
- Huang, G., Jiang, K., Payne, M.G., Deng, L.: Formation and propagation of coupled ultraslow optical soliton pairs in a cold three-state double- Λ -system. *Phys. Rev. E* **73**, 056606 (2006)
- Imamoglu, A., Harris, S.E.: Lasers without inversion: interference of dressed lifetime broadened states. *Opt. Lett.* **14**, 1344–1346 (1989)
- Ishikawa, H.: *Ultrafast All-Optical Signal Processing Devices*. Wiley, Singapore (2008)
- Islam, K., Bhattacharyya, D., Ghosh, A., Biswas, D., Bandyopadhyay, A.: Study on probe field propagation in the presence of control and coupling fields through a four-level N-type atomic system. *J. Phys. B At. Mol. Opt. Phys.* **50**, 215401 (2017)
- Jafarzadeh, H.: All-optical switching in an open V-type atomic system. *Laser Phys.* **27**, 025204 (2017)
- Joshi, A., Xiao, M.: Electromagnetically induced transparency and its dispersion properties in a four-level inverted-Y atomic system. *Phys. Lett. A* **317**, 370–377 (2003)
- Joshi, A., Xiao, M.: Vacuum Rabi splitting for multilevel electromagnetically induced transparency system. *Eur. Phys. J. D* **30**, 431–439 (2004)
- Joshi, A., Xiao, M.: Generalized dark-state polaritons for photon memory in multilevel atomic media. *Phys. Rev. A* **71**, 041801 (2005)
- Khoa, D.X., Doai, L.V., Son, D.H., Bang, N.H.: Enhancement of self-Kerr nonlinearity via electromagnetically induced transparency in a five-level cascade system: an analytical approach. *J. Opt. Soc. Am. B.* **31**, 1330–1334 (2014)
- Khoa, D.X., Trong, P.V., Doai, L.V., Bang, N.H.: Electromagnetically induced transparency in a five-level cascade system under Doppler broadening: an analytical approach. *Phys. Scr.* **91**, 035401 (2016)
- Khoa, D.X., Trung, L.C., Thuan, P.V., Doai, L.V., Bang, N.H.: Measurement of dispersive profile of a multi-window EIT spectrum in a Doppler-broadened atomic medium. *J. Opt. Soc. Am. B.* **34**, 1255–1263 (2017a)

- Khoa, D.X., Dong, H.M., Doai, L.V., Bang, N.H.: Propagation of laser pulse in a three-level cascade inhomogeneously broadened medium under electromagnetically induced transparency conditions. *Optik* **131**, 497–505 (2017b)
- Li, J., Yu, R., Si, L., Yang, X.-X.: Propagation of twin light pulses under magneto-optical switching operations in a four-level inverted-Y atomic medium. *J. Phys. B At. Mol. Opt. Phys.* **43**, 065502 (2010)
- Qi, Y., Zhou, F., Yang, J., Niu, Y., Gong, S.: Controllable twin laser pulse propagation and dual-optical switching in a four-level quantum dot nanostructure. *J. Opt. Soc. Am. B* **30**, 1928–1936 (2013)
- Rajitha, K.V., Tarak, N.D., Jorg, E., Martin, K.: Pulse splitting in light propagation through N-type atomic media due to an interplay of Kerr nonlinearity and group-velocity dispersion. *Phys. Rev. A* **90**, 023840 (2015)
- Schmidt, H., Ram, R.J.: All-optical wavelength converter and switch based on electromagnetically induced transparency. *Appl. Phys. Lett.* **76**, 3173–3175 (2000)
- Sheng, J., Yang, X.-H., Khadka, U., Xiao, M.: All-optical switching in an N-type four-level atom-cavity system. *Opt. Express* **19**(18), 17059–17064 (2011)
- Si, L.G., Lu, X.Y., Hao, X., Li, J.H.: Dynamical control of soliton formation and propagation in a Y-type atomic system with dual ladder-type electromagnetically induced transparency. *J. Phys. B At. Mol. Opt. Phys.* **43**, 065403 (2010)
- Steck, D.A.: Rubidium 87 D Line Data, available online at <http://steck.us/alkalidata> (revision 2.2.2, 9 July 2021)
- Wang, H., Goorskey, D., Xiao, M.: Enhanced Kerr nonlinearity via atomic coherence in a three-level atomic system. *Phys. Rev. Lett.* **87**, 073601 (2001)
- Wang, H., Goorskey, D., Xiao, M.: Controlling light by light with three-level atoms inside an optical cavity. *Opt. Lett.* **27**, 1354–1356 (2002)
- Yang, X., Li, S., Zhang, C., Wang, H.: Enhanced cross-Kerr nonlinearity via electromagnetically induced transparency in a four-level tripod atomic system. *J. Opt. Soc. Am. B* **26**, 1423–1434 (2009)

Publisher's Note Springer Nature remains neutral with regard to jurisdictional claims in published maps and institutional affiliations.